Доклади на Българската академия на науките
Comptes rendus de L' Academie bulgare des Sciences
Tome 51, N° 1-2, 1998

ASTRONOMIE

SPECTRAL ANALYSIS OF SEYFERT 1 GALAXIES

L. Slavcheva, G.Petrov, B. Mihov

(Submitted byAcademician V. Andrejtscheff on February 18, 1997)

I. INTRODUCTION

Broad HI, HeI, HeII emission lines are typical for Seyfert 1 galaxies (Sy1 Gs). The observed permitted lines are roughly symmetric. They can be regarded as arising from the collective motions of an ensemble of clouds ([1]).

Optically thin clouds can be efficiently accelerated by UV radiation, assuming $g_{r,\,uv} >> g_{r,\,x}$. In the absence of strong drag forces the equation of motion is independent of the cloud mass M_c :

$$\frac{du}{dt} = \frac{u^2}{R} \equiv g_{r,uv} \equiv \frac{udu}{dR} = \frac{n\alpha\phi h\nu_0}{m_p c}, \qquad (1)$$

where u is the cloud radial velocity, R is the distance of the emitting regions from the central source of radiation, n is the density, m_p is the proton mass and $\phi = 2$ roughly corrects for the presence of He and represents the ratio of the Rydberg energy $h\nu_0$ to the mean photon energy.

The specific photon luminosity of an emission line L_ν with angle $\theta = \arccos \mu$ between the velocity of the cloud and the line of sight for the blue ($\mu>1$) side of the symmetric line is:

$$L_\nu = \int_{R_0}^{\infty} dR \int_0^1 d\mu \delta[\nu - \nu_l(1+\frac{u}{c}\mu)]\varepsilon_c n_c 2\pi R^2 . \qquad (2)$$

Here $\nu_l=(1+\mu u/c)$ is the Doppler shifted observed frequency and $\varepsilon_c=n\alpha_l M_c/m_p$ is the number of photons produced per second per each cloud.

$$L_\nu = \frac{\dot{M}_c \alpha_l c}{2 m_p \nu_l} \int_{cx}^{\infty} \frac{n}{u^2} \left|\frac{dR}{du}\right| du = \left(\frac{\dot{M}_c c^2 \alpha_l}{\nu_l h\nu_0 \alpha}\right) \int_{cx}^{\infty} \frac{du}{u} \equiv \Lambda \ln \frac{u_{max}}{cx} . \qquad (3)$$

Equation (3) expresses the logarithmic (ln) line profile in dimensionless frequency displacement from the center $x = (\nu - \nu_l)/\nu_l$ ([2], [3]). The maximum velocity u_{max} arises from a terminal velocity if the cloud density varies as R^{-s} with $s>1$ ([4]).

There is a tendency for the FWHMs in Sy1 nuclei to be correlated with the ionization potential in the sense that ions with higher ionization potential have larger FWHM. Under the assumption :

$$N_e \sim r^{-m}, \qquad (4)$$

the ionization parameter at the face of the cloud is:

$$\Gamma = \frac{Q(H^0)}{4\pi r^2 c n_e} \propto r^{-2}, \qquad (5)$$

where $Q(H^0)$ is the number of ionizing photons emitted by the central source per unit time. Therefore Sy1 Gs tend to have $m \approx 0$, i.e.

$$\Gamma \sim r^{-2}. \qquad (6)$$

Some of the forbidden line profiles show asymmetry ([5]). If emitting material velocities were dominated by orbital or random motions, a random distribution of line asymmetries would

be likely. The predominance of blue line wings stronger than red ones in narrow emission line data suggest radial motion as well as obscuration.

II. OBSERVATIONS AND REDUCTION OF THE SPECTRAL DATA

Some of the spectral data were taken with the 2.6-m telescope at the Crimean Astrophysical Observatory with dispersion 90 A.mm^{-1}, the others were taken with the 2-m telescope at the NAO "Rozhen" with dispersion 50 A.mm^{-1}.

The reduction was done with the software MIDAS of the ESO.

The reduction of the raw data to a relative intensity versus scale involved several major steps:

1. Instrument calibration: linearization of the spectral data;
2. Separation of the object spectrum, the comparison spectrum and the night sky spectrum from the raw one; subtraction the night sky spectrum and the plate background from the object spectrum and from the comparison one;
3. Wavelength calibration:

a) identification of the lines in the comparison spectrum;
b) transformation pixel-wavelength in the comparison spectrum;
c) transformation pixel-wavelength in the object spectrum;
d) estimation of the redshift in the object spectrum.

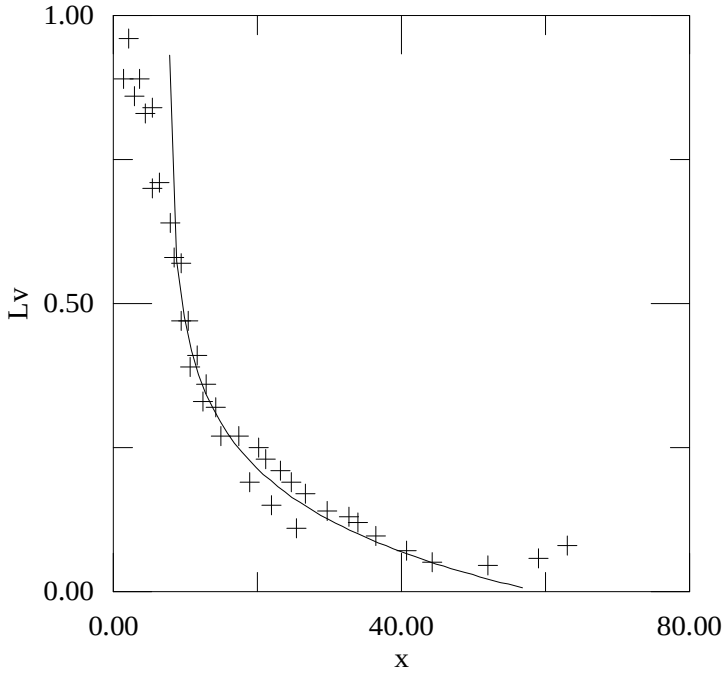

Figure 1

III. RESULTS

1. The observed Hβ profiles are symmetric and can well be fitted with a ln profile, except of a narrow nuclear region:

$$L_v \sim \ln(|x|^{-1}). \quad (7)$$

The result of such an approximation is shown in Figure 1 for the galaxy Akn 564.

Outward radial motions of optically thin and therefore isotropically emitting clouds is a mechanism of formation of ln profiles.

Ln line profiles can however result in any physical situation for which:

$$\varepsilon_c n_c \pi R^2 \sim udu, \quad (8)$$

where ε_c is the filling factor ([6]). This is consistent with the applicability of the ln profile calculations in the optically thick limit.

Orbital motions of gravitationally bound clouds in nearly circular orbits around the central object can explain the ln broad line profiles. The main problem is that the whole cloud is sheared by differential Poynting - Robertson forces in a time comparable or less than the orbital period and the cylindrically deformed cloud of fully ionized gas can no longer radiate lines characteristic of the partially ionized zone (MgII, Hα , FeII, etc.).

Line profiles similar to the observed ln shapes can be also generated by emission from a rotating disk. Such models are contradictionary as they require the central part of the line profile be strongly depressed due to self-absorption and the source of ionizing radiation be above the disk rather than located near the central mass.

In the presence of strong drag forces outward moving clouds would pass through a maximum velocity and would produce two overlapping line profiles as they are first accelerated, then - decelerated. The combined line profile would in general be non-ln.

In spite of the variety of physical situations which can generate symmetric ln broad line profiles, the situations in rough contradiction with lots of observations and the observed continuity and smoothness of the profiles shape put some restrictions on the models: the most probable and successful is the model of radially outward moving clouds in a hot intercloud medium lacking dominant drag forces.

Table 1

Ion	λ, A	χ, eV	FWHM Mrk871	FWHM N7469	FWHM Mrk1040	FWHM M81111
[SII]	6730.74	1.83	-	575±22	442±22	-
[SII]	6716.52	1.84	492±22	591±22	357±22	-
[OI]	6300.31	1.96	671±24	-	514±24	596±24
[OI]	6363.82	1.96	-	709±23	487±23	464±23
[OIII]	4958.95	2.50	1070±30	-	-	1107±30
[OIII]	5006.88	2.50	921±30	-	-	1290±30

Remark: [FWHM]=km.s^{-1}. Lack of data should mean either a weak line or a line blended with other lines.

2. Our results about five objects confirm the correlation FWHM ~ χ, cited by a great deal of authors (Table 1).

The highest ionization occurs closest to the central source; hence, the highest internal velocities occur there. Having in mind that in a structure with a wide range of electron densities n_e , the region with $n_e \sim n_e^{cr}$ of any energy level is the most effective in the emission of the line arising in that level and the correlation FWHM ~ n_e^{cr} for Sy2 Gs, we accept a model of outwardly decreasing velocities and an ionization parameter $\Gamma \sim r^{-2}$.

3. We introduce a set of measures to describe quantitatively the forbidden line profile asymmetries and the FWHM ([5]):

a) W_{20}, W_{50}, W_{80} ([km.s^{-1}]), defined in terms of the velocity positions respectively at 20%, 50%, 80% of the full height: $W_{20} = V_7 - V_6$, $W_{50} = V_6 - V_2$, $W_{80} = V_5 - V_3$ (Figure 2);

b) shifts of the line centers at the 20% (C_{20}), 50% (C_{50}) and 80% (C_{80}) levels from the line peak positions: $C_{20} = (V_1 + V_7)/2 - V_4$, $C_{50} = (V_2 + V_6)/2 - V_4$ and $C_{80} = (V_3+V_5)/2 - V_4$.

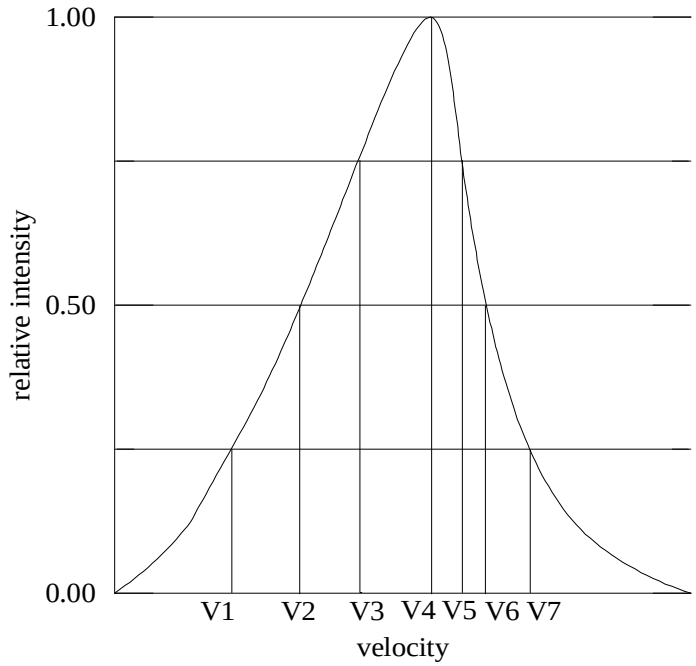

Figure 2

Table 2

Obj., Line	W_{20}/W_{50}	W_{80}/W_{50}	C_{20}/W_{50}	C_{50}/W_{50}	C_{80}/W_{50}
M81111, [OIII]5007	1.638 ±0.076	0.560 ±0.044	−0.068 ±0.030	−0.032 ±0.029	−0.038 ±0.029
Akn 564, [OIII]4959	1.559 ±0.128	0.573 ±0.080	−0.196 ±0.060	−0.056 ±0.053	−0.022 ±0.051
Mrk 876, [OIII]4959	1.861 ±0.136	0.515 ±0.072	−0.637 ±0.078	−0.130 ±0.054	−0.001 ±0.047

We use the scaled (dimensionless) measures W_{20}/W_{50}, W_{80}/W_{50}, C_{20}/W_{50}, C_{50}/W_{50}, C_{80}/W_{50}.

Quantitative estimates in terms of the above introduced measures of [OIII] λ4959 and [OIII] λ5007 for the galaxies MCG 8-11-11, Akn 564 and Mrk 876 are given in Table 2. We find good accordance with the results got in [5]. Not being able to serve as a base for deductions because of their small number, the analyzed spectral data confirm the lack of systematic offset between the velocity of the line peak and the velocity of the galaxy ([5], [7]). Most attention has been paid to [OIII] λ5007 because it is the brightest unblended optical narrow line.

The observed asymmetric profiles with wings extending to the blue can be understood as resulting from extinction by dust and outward flowing ionized gas: line photons emitted on the more distant side of the structure will pass through more dust on their way to us and will suffer more extinction; as the further side is moving away from us, there will be fewer photons observed from the red side of the profile than the blue one.

In fine, the least contradictionary model of the BLR includes a radial outward flow of clouds of ionized gas in a low-pressure hot intercloud medium. Ionizing radiation from a central source is limited to a biconical region, the remainder being blocked by an optically thick accretion disk. Highest internal velocities and highest potentials of ionization occur in the vicinity of the central source. Photoionization is the main energy-input mechanism that can produce the wide range of ionization observed among the narrow forbidden lines. The asymmetry of several forbidden line profiles observed involve outward flow and extinction by dust distributed in any fashion in the central plane.

REFERENCES

[1] Mathews W., 1974, ApJ, 189, 23. [2] Blumenthal G., Mathews W., 1975, ApJ, 198, 517. [3] Blumenthal G., Mathews W., 1979, ApJ, 233, 479. [4] Mathews W., Capriotti E., 1985, Conference on Astrophysics of AGN and QSOs, edited by J.S.Miller, p.185. [5] Vrtilek J., Carleton,N., 1985, ApJ, 294, 106. [6] Capriotti E., Foltz C., Byard P., 1980, ApJ, 245, 396. [7] Mirabel I., Wilson A., 1984, ApJ, 277, 92.

Insitute of Astronomy
Bulgarian Academy of Sciences
72, Tsarigradsko chaussee Blvd
1784 Sofia, Bulgaria